Applied Surface Science 29 (1987) 341–360
North-Holland, Amsterdam

ADSORPTION-INDUCED CONDUCTANCE CHANGES OF THIN Pt FILMS AND PtPd/TiO_2 GAS SENSORS

Ambesh G. SHASTRI and Johannes SCHWANK *

Department of Chemical Engineering, The University of Michigan, Ann Arbor, MI 48109-2136, USA

Received 13 May 1987; accepted for publication 27 June 1987

Chemisorption of H_2 and O_2 and resulting changes in electrical conductance of a typical gas sensing material, PtPd/TiO_2, and thin Pt films on glass are studied and compared. The activation energy of conduction increases as Pt film thickness decreases. Chemisorption of H_2 on thin Pt films causes an increase in conductance and activation energy of conduction. O_2 chemisorption results in a decrease in conductance and increase in activation energy of conduction. Alteration in the number of charge carriers and reduction in charge carrier mobility are the mechanisms proposed for the observed changes. Compared to thin Pt films, relatively large changes in electrical conductance are observed upon chemisorption of gases on TiO_2 supported PtPd. The role of the oxide substrate in the observed chemical interaction and electronic response is discussed. The electronic changes upon adsorption/desorption of gases are reversible for thin Pt films but only partially reversible for TiO_2 supported PtPd.

1. Introduction

Considerable research efforts have been directed towards the development of semiconductors as gas sensors for various applications. Titania has been studied as an oxygen sensor for use in nonequilibrium gas mixtures composed of combustible gas, O_2 and N_2. Sensors of this type are applied for controlling the air/fuel ratio in automobile catalytic converters [1,2]. Catalytic additives such as Pt and Pd are often used to obtain a higher sensitivity in gas sensing [3,16,17]. These metals are generally deposited in form of small particles on the surface of the TiO_2 substrate. Typical TiO_2 substrates consist of sintered oxide grains connected by thin necks which represent the conductance controlling features of the oxide [4]. The correlation between the microstructure of such sensor materials and their electronic response to gas adsorption is still an active area of research. Changes of activation energy and/or Fermi energy level due to chemisorption of gases need to be carefully examined to arrive at a better understanding of gas sensing materials. The interaction between

* To whom correspondence should be addressed.

sensor surface and adsorbate gas can lead to changes in electron density, and an optimum Fermi energy level is necessary to facilitate such electronic effects. Information about the Fermi energy level can be obtained by in situ electrical conductivity studies.

Charge carrier transport through discrete, small metal particles has been the subject of numerous investigations. The electrical conduction mechanism in thin, discontinuous metal films has been explained on the basis of thermionic emission and/or activated tunneling [5,6]. For particles separated by less than 8 nm, thermionic emission dominates the electrical conductivity at temperatures exceeding 300 K [5]. Activated tunneling has been proposed as the main mechanism of conduction at temperatures lower than 300 K [8]. It has also been suggested that a certain number of microparticles must be charged (or ionized) before tunneling can take place, with tunneling occurring between the charged and uncharged microparticles. Metal films (< 10 nm) are generally discontinuous and display greatly reduced electrical conductivity [6–8]. Due to the high surface to volume ratio of such thin films, chemisorption of gases can strongly influence the electrical conduction. For example, it has been reported that oxygen chemisorption on thin copper [9] and silver [10] films leads to an increase in the electrical resistance. Three possible mechanisms for the influence of oxygen chemisorption on thin copper and silver films have been considered, namely, (a) decrease in the effective thickness of the film due to formation of a surface complex, (b) variation in the number of conduction electrons of the metal, (c) reduction in charge carrier mobility due to increased scattering at the surface by the presence of adsorbed species [11]. Various models have been proposed for the interaction between adsorbed species and conduction electrons of thin metal films with major emphasis on scattering of electrons by adatoms [12,13]. The concept of chemisorption-induced demetallization has been of considerable debate between various research groups [14,15]. Demetallization is the effective decrease in metal thickness due to localized bonding at the surface. It is conceivable that the demetallization effect is manifested to a different extent on different properties such as conductivity. Hall effect and magnetic coupling [15].

Our objectives of this study were to investigate adsorption induced conductivity changes on glass supported Pt thin films of varying thickness, blank TiO_2, $PtPd/TiO_2$, and to critically evaluate the differences between the three systems. $PtPd/TiO_2$ is studied here as a typical gas sensor and was prepared so that the metal is in the form of isolated metal islands distributed on the surface of TiO_2 powder particles. The results obtained on this gas sensor, $PtPd/TiO_2$, are then compared with those obtained on discontinuous thin Pt films on glass substrates. It is important to note that the metal in both systems is in the form of discrete islands on the underlying substrate material. Due to the low Pd content in $PtPd/TiO_2$ and the similarity of these two metals in terms of their electronic response to gas adsorption, it is justified to compare

$PtPd/TiO_2$ with monometallic Pt films on glass. The thin film study provides an understanding of the role of film thickness and metal particle size on changes in electronic response caused by chemisorption of gases. Comparison of the adsorption induced electronic response of thin metal films on glass, which is an insulator, with that of metal supported on TiO_2 which is an n-type semiconductor permits an evaluation of the role of the substrate.

2. Experimental

2.1. Sample preparation

Thin Pt films on glass substrates (15 mm × 15 mm) were prepared by using an Energet electron beam deposition system. Prior to metal deposition, the glass substrates were carefully cleaned and outgassed. An ultrahigh purity metal source and high system-vacuum was used to avoid sample contamination. An average deposition rate of 1 nm/s was used and the film thickness was continuously monitored. The substrate temperature during deposition was 310 K. Three Pt films with nominal thicknesses of 5, 10, and 20 nm, respectively, were prepared. In all three cases, the metal was deposited in forms of discrete islands with increasing average particle size as the film thickness increased.

$PtPd/TiO_2$ was prepared by wet impregnation of blank TiO_2 powder with appropriate aqueous precursor metal salt (H_2PtCl_6, $(NH_4)_2PdCl_4$) solutions followed by washing, drying and hydrogen reduction steps. The metal content of the sample was determined by neutron activation analysis as 1.31 wt% Pt and 0.16 wt% Pd. The BET surface area of blank TiO_2 and the $PtPd/TiO_2$ sample was measured to be 0.25 ± 0.05 m^2/g. For conductance measurements, the TiO_2 and the $PtPd/TiO_2$ powders were pressed into the form of chips, 3 mm × 1 mm.

2.2. Experimental set-up

The samples were mounted in a custom built high vacuum, pyrex glass chamber. This high vacuum chamber was equipped with quartz-shielded heating cartridges controlled by an Omega PID temperature programmer with linear heating ramp and soak programs. This heating method provided radiative heating of the sample without introducing any noise in the electrical conductivity measurements. The temperature of the film was monitored by a glass-shielded thermocouple which was located immediately below the sample. The high vacuum chamber was connected to a static, volumetric chemisorption system equipped with ion gauge, thermocouple gauge, and solid-state pressure transducer for monitoring the pressure.

The samples were connected on all four corners with high conducting silver epoxy to four Au wires of 0.5 mm diameter which were connected to the external circuit via high vacuum feed-throughs. Conductivity measurements were carried out using two diagonally opposite Au contacts and then repeated with the other two diagonally opposite contacts in order to check for contact artifacts. A phase-sensitive external circuit consisting of a variable frequency function generator (Krohn–Hite Model 1600) and lock-in amplifier (Ithaco Model 393) with high precision resistors was employed. A block diagram of the external circuit is given in fig. 1. The output from the function generator and lock-in amplifier, temperature and pressure were continuously monitored using a computer-controlled eight channel data acquisition system. The lock-in amplifier monitored the voltage across the sample which was in phase with that from the function generator and standard resistor. Any out of phase signal due to capacitance, thermal EMF's or DC component was thus effectively eliminated. A sine wave of 100 Hz frequency and 10 V amplitude from the function generator and suitable precision resistors between 10^4 and 10^8 Ω were used in the experiments.

After loading the sample, the vacuum chamber was evacuated at room temperature for four hours. The sample temperature was linearly ramped up to 523 K with a heating rate of 1.5 K/min under dynamic vacuum and kept at 523 K for an additional four hours. Then, the sample was cooled down to 298 K under vacuum. Following this outgassing treatment, the conductivity measurements were carried out using different combinations of Au contacts. First, the electrical conductance of the outgassed sample was monitored as a function of temperature while the sample was kept under dynamic vacuum. The sample was then exposed to a dose of H_2 gas at 298 K, so that an equilibrium pressure of about 800 Pa resulted after 0.5 h. Electrical conduc-

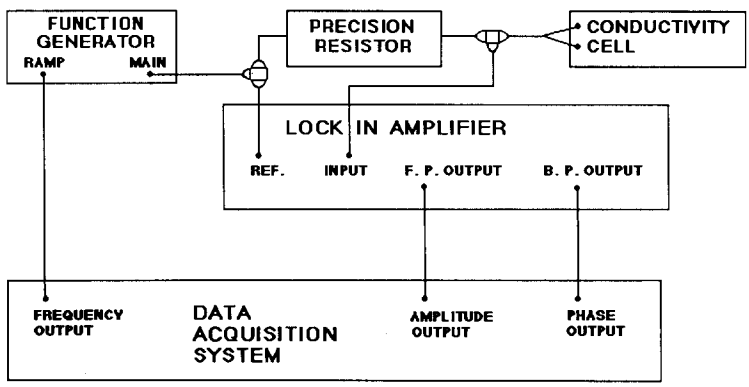

Fig. 1. Block diagram showing various components of external circuit for electrical conductivity measurements.

tance was then measured as a function of temperature, after allowing 0.5 h for equilibrium in 800 Pa of H_2 at each temperature. For each temperature, conductance was also measured after evacuation of H_2 for 2 h. Following a similar procedure, the adsorption of oxygen at a pressure of 800 Pa was studied on blank TiO_2, $PtPd/TiO_2$, and 20 nm Pt film/glass. The pressure dependence of electrical conductance was not studied in view of the small surface areas of the samples and the small amounts of gas adsorption on the samples investigated.

In order to understand the microstructure of the $PtPd/TiO_2$ gas sensor, electron microscopy studies were carried out in a JEOL-100CX TEM/STEM instrument equipped with a side-entry goniometer stage, an ASID-4D scanning attachment and a lithium-drifted solid-state X-ray detector for elemental analysis. For data acquisition and analysis, a multichannel analyzer connected to a ND6620 computer was used. Specimen preparation was done by placing a droplet of powder suspension in isopropanol onto a copper grid covered with a porous carbon film. A suitable sampling area was first identified and photographed in the transmission made and then the microscope was switched over to the scanning transmission mode for energy dispersive X-ray spectroscopy (EDS). A 10 nm electron probe and X-ray counting time of 200 s was used for EDS. Microdiffraction patterns were obtained by using a condenser aperture of 20 μm. Camera length calibration was carried out for specific values of lens current and specimen position using a polycrystalline Au standard. X-ray diffraction studies were performed in a Philips X-ray diffractometer with monochromatic Cu Kα as radiation source to gain information about the crystal phases and metal particle sizes.

3. Results and discussion

3.1. Electrical conductance of thin Pt films on glass

Fig. 2 shows the conductance of Pt films of varying thickness as a function of reciprocal temperature in vacuum and upon exposure to H_2 gas. Also shown are data concerning O_2 adsorption on 20 nm Pt/glass. Activation energies of conductance can be obtained from Arrhenius plots and the expression

$$G_i = G_0 \exp(-E/kT_i) \tag{1}$$

following the analysis of Hartman [6]. G_i is the sample conductance at temperature T_i, E represents the activation energy and k is Boltzmann's constant. For better accuracy in the computation of activation energies, the data presented in fig. 2 have been normalized with respect to a reference

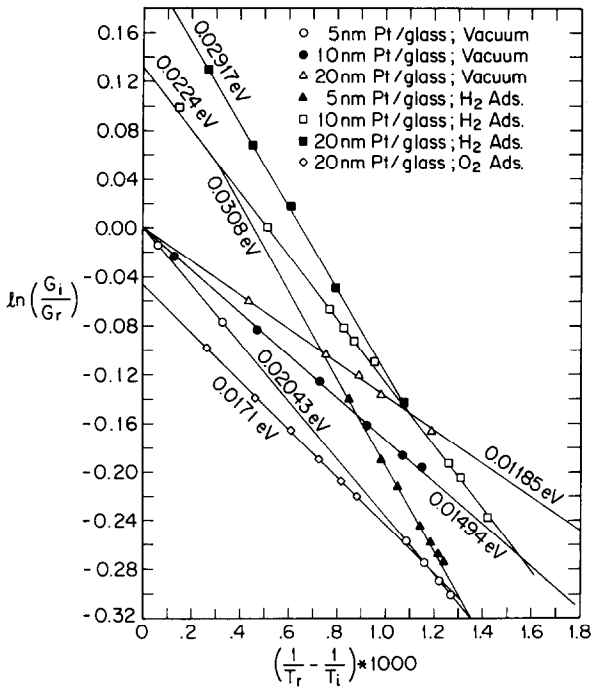

Fig. 2. Arrhenius plots representing normalized data of electrical conductance as a function of reciprocal temperature for thin Pt films on glass. G_i and G_r are the sample and reference conductance for a given film corresponding to temperatures T_i and T_r respectively. 5 nm Pt/glass: $T_r = 351$ K, $G_r = 0.0192\ \Omega^{-1}$; 10 nm Pt/glass: $T_r = 347$ K, $G_r = 0.0521\ \Omega^{-1}$; 20 nm Pt/glass; $T_r = 303$ K, $G_r = 0.1354\ \Omega^{-1}$.

conductance, G_r, of the thin film samples in vacuum, at temperature T_r, following the relations

$$G_r = G_0 \exp(-E/kT_r), \tag{2}$$

$$\frac{G_i}{G_r} = \exp\left[\frac{-E}{k}\left(\frac{1}{T_r} - \frac{1}{T_i}\right)\right]. \tag{3}$$

A plot of ln (G_i/G_r) versus $(1/T_r - 1/T_i)$ as shown in fig. 2 permits a determination of the activation energy of conductance. The results are summarized in table 1. For the vacuum treated Pt films, the activation energy of conductance decreased with increasing film thickness in agreement with theoretical predictions that the conductance of thin discontinuous metal films should depend exponentially on the reciprocal temperature over a reasonably large temperature range and that there should be a marked dependence of the activation energy on film thickness and particle size [8]. The lower conduc-

Table 1
Activation energies of conductance and temperature coefficients of resistance of thin Pt films on glass after treatment in vacuum, H_2, and O_2

Film thickness (nm)	Activation energy of conductance (eV) (± 0.001 eV)			Temperature coefficient of resistance (K^{-1}) ($\pm 0.5\times10^{-4}$)		
	Vacuum	H_2	O_2	Vacuum	H_2	O_2
5	0.020	0.031	–	6.6×10^{-4}	13.5×10^{-4}	–
10	0.015	0.022	–	8.7×10^{-4}	17.2×10^{-4}	–
20	0.012	0.029	0.017	10.9×10^{-4}	28.1×10^{-4}	15.1×10^{-4}

tance and higher activation energy of thin films as compared to bulk metal can be attributed to the shortened mean free path of electrons due to the limited thickness and restricted geometry of the metal islands. The activation energy of conductance in such thin films can be assumed to be independent of applied electric fields, at least in the limit of small fields of about 10 V/cm.

The temperature coefficients of resistance, α

$$\alpha = \frac{R - R_0}{R_0}\frac{1}{T - T_0}, \tag{4}$$

of the three Pt films for a temperature range of 373–623 K are also listed in table 1. The temperature coefficients of resistance are positive, and with increasing film thickness the value of α increases. However, for all three films the values of α are significantly lower than the bulk value for Pt of 39.27×10^{-4} K^{-1} [23].

On all three films, adsorption of H_2 caused an increase in conductance. The increase can be attributed to charge transfer from chemisorbed hydrogen atoms to the conduction band of Pt. Hydrogen chemisorption on Pt is known to decrease the work function of the metal [19] and increase the charge carrier concentration. Additional evidence for the increase in charge carrier concentration due to hydrogen adsorption is provided by the large increase in the temperature coefficients of resistance, α (see table 1).

However, in spite of an increase in charge carrier concentration, the activation energy of conductance increased upon H_2 adsorption on the three Pt films.For the 5 and 10 nm Pt film, the activation energies increased by a factor of 1.5, as compared to much larger increase by a factor of about 2.5 for the 20 nm Pt film. The relative changes in the activation energy of conductance on each of the three Pt films seem to depend not simply on film thickness, but in a more complex manner on the details of sample morphology and surface concentration of adsorbed hydrogen. The increase in activation energy indicates that reduced charge carrier mobility plays a major role in influencing the conduction in hydrogen covered thin Pt films.

Thus, two counteracting mechanisms appear to influence the conductance change induced by hydrogen adsorption: (a) an increase in charge carrier

concentration due to the donor gas nature of H_2 and (b) a reduction in charge carrier mobility due to increased scattering of electrons by adsorbed species.

Adsorption of oxygen, which is an acceptor gas capable of capturing conduction band electrons and injecting holes into the conduction band of metals, significantly reduced the conductance of the 20 nm Pt film and increased the activation energy of conductance (fig. 2, table 1). As in the case of hydrogen adsorption the increase in activation energy can be attributed to increased electron scattering by adsorbed oxygen atoms resulting in decreased charge carrier mobility. The temperature coefficient of resistance, α, increased by about 50% upon oxygen adsorption.

The gas adsorption induced conductance changes were completely reversible, and the original conductance and activation energy values of the vacuum treated films could be restored upon removal of the adsorbed hydrogen or oxygen species through evacuation at high temperatures.

3.2. Electrical conductance of TiO_2 and $PtPd/TiO_2$

Prior to investigating the effect of H_2 and O_2 adsorption on the electrical conductance of TiO_2, the powders were characterized by X-ray diffraction and electron microscopy to gain insight into their morphology, particle size distribution, and microstructure. The TiO_2 support consisted of the rutile phase of titania, as shown by X-ray diffraction. The $PtPd/TiO_2$ sample also contained the rutile phase of TiO_2, and X-ray diffraction gave characteristic peaks for Pt. No X-ray peaks attributable to Pd were observed which is not surprising in view of the low Pd metal loading. From Scherrer's equation for X-ray line broadening of the Pt(111) peak, corrected for instrumental contributions, an average Pt metal particle size of 29.8 nm was calculated. This metal particle size is in qualitative agreement with the volumetric average metal particle size, $d_v = 38.2$ nm obtained from transmission electron microscopy according to the equation

$$d_v = \frac{\Sigma n_i d_i^4}{\Sigma n_i d_i^3}, \tag{5}$$

where d_i represents the diameter of a given metal particle, and n_i the number of particles within a given size range d_i. A representative bright field transmission electron micrograph of $PtPd/TiO_2$ is shown in fig. 3 and the metal particle size distribution obtained from several such micrographs is given in fig. 4. Fig. 4 also indicates the number average particle size, d_n, and surface average particle size, d_s, calculated by using

$$d_n = \frac{\Sigma n_i d_i}{\Sigma n_i}, \tag{6}$$

$$d_s = \frac{\Sigma n_i d_i^3}{\Sigma n_i d_i^2}. \tag{7}$$

Fig. 3. Bright field transmission electron micrograph of $PtPd/TiO_2$.

The elemental composition of small sample regions was determined by energy dispersive spectroscopy (EDS) where the electron beam is focused onto a region of interest, and the energy of the emitted X-rays is analyzed. This technique allows to distinguish between sample regions containing metal and metal-free regions containing only the TiO_2 substrate. It is also possible to focus the beam onto an individual metal particle and to qualitatively determine the elemental composition. The low X-ray counts achieved from individual, small metal particles preclude a statistically significant quantitative analysis.

Scanning the electron beam over regions of low contrast in $PtPd/TiO_2$ resulted in strong X-ray signals for titanium. Focusing the beam on regions of high contrast, about 10 nm in diameter, showed the presence of Pt and Pd. Most of the metal particles examined by EDS contained both Pt and Pd. Figs. 5 and 6 show two typical EDS spectra from the sample $PtPd/TiO_2$. Microdif-

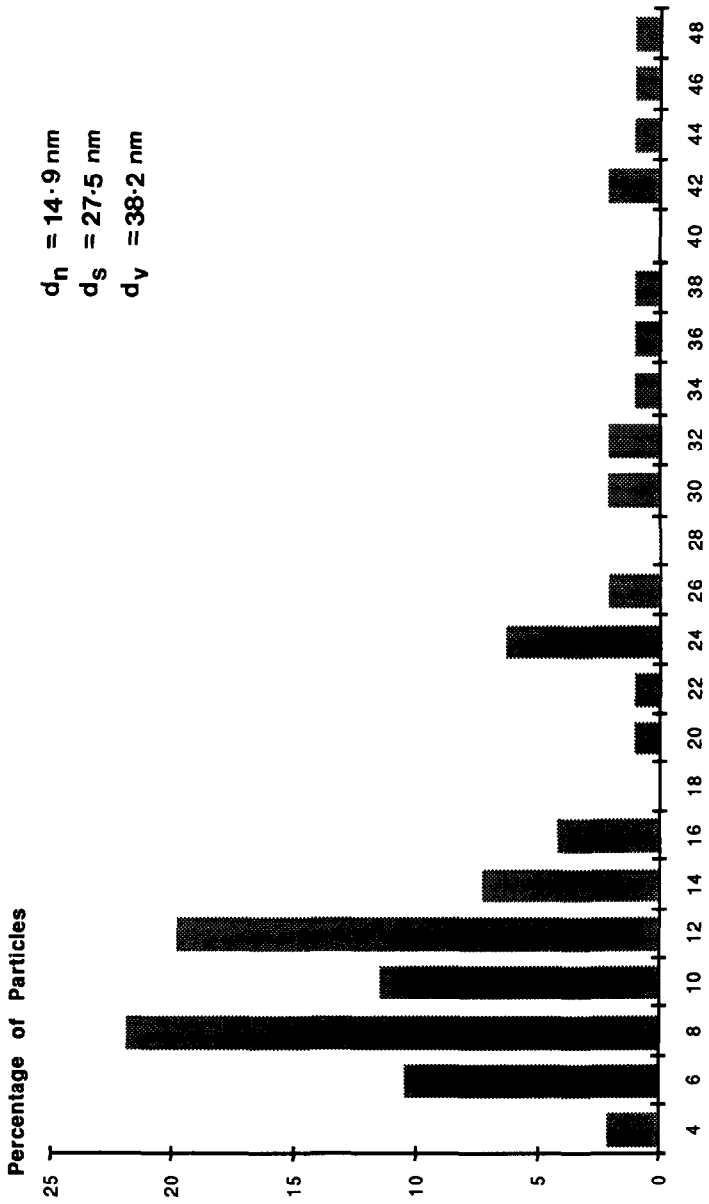

Fig. 4. Histogram showing metal particle size distribution of $PtPd/TiO_2$.

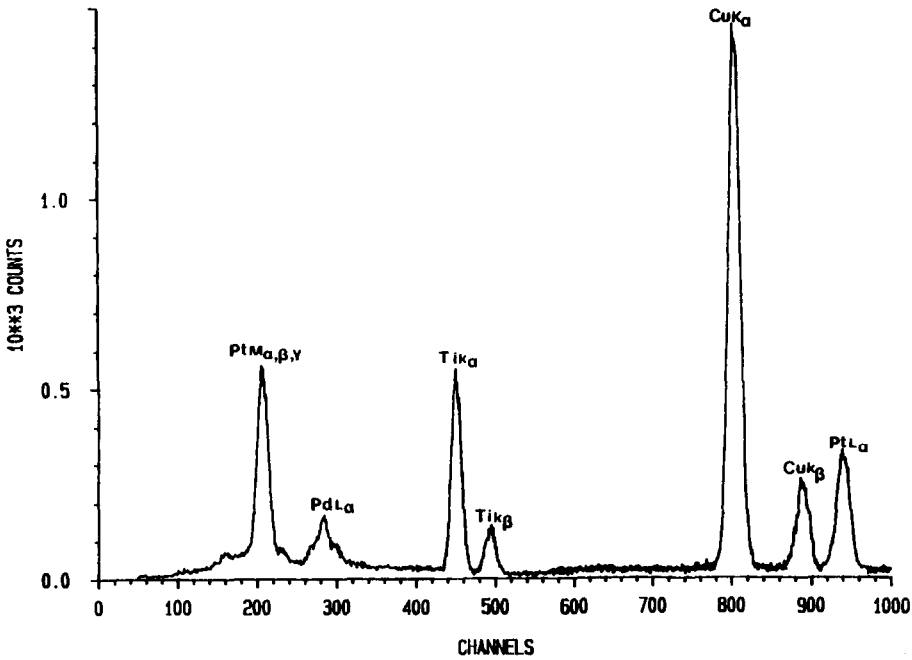

Fig. 5. EDS spectra of $PtPd/TiO_2$ showing the presence of Pt and Pd in a single particle (size = 8 nm). Cu peaks in the spectra arise from the grids used to support the specimen.

fraction patterns of individual metal particles were obtained in order to gain structural information. Ring patterns were observed from metal particle free regions and were attributable to the rutile phase of TiO_2 (fig. 7a). Microdiffraction patterns from metal particles showed the presence of Pt–Pd (fig. 7c) and Pt particles (figs. 7b, d and e). The metal particles were randomly aligned on the oxide substrate with different planes exposed on the surface. Some particles showed multiple twinning (fig. 7f). The structural details of $PtPd/TiO_2$ show that the metal is present in the form of discrete islands.

The electrical conductance of oxide samples with and without surface additives has been investigated by a number of researchers for example, Morrison [18,20], and Herrmann [21,22]. The measurement of relative conductance changes of a pressed pellet as a function of temperature permits the determination of the Fermi energy of the metal-containing sample relative to the conduction band minimum of blank TiO_2. Following previous work by Morrison [20], the conductance in such systems can be analyzed by the expression,

$$G = \mu f(A) g(d) e N_c \exp\left[-(E_{cs} - E_F)/kT\right], \tag{8}$$

where μ is the electron mobility, $f(A)$ and $g(d)$ are geometric factors

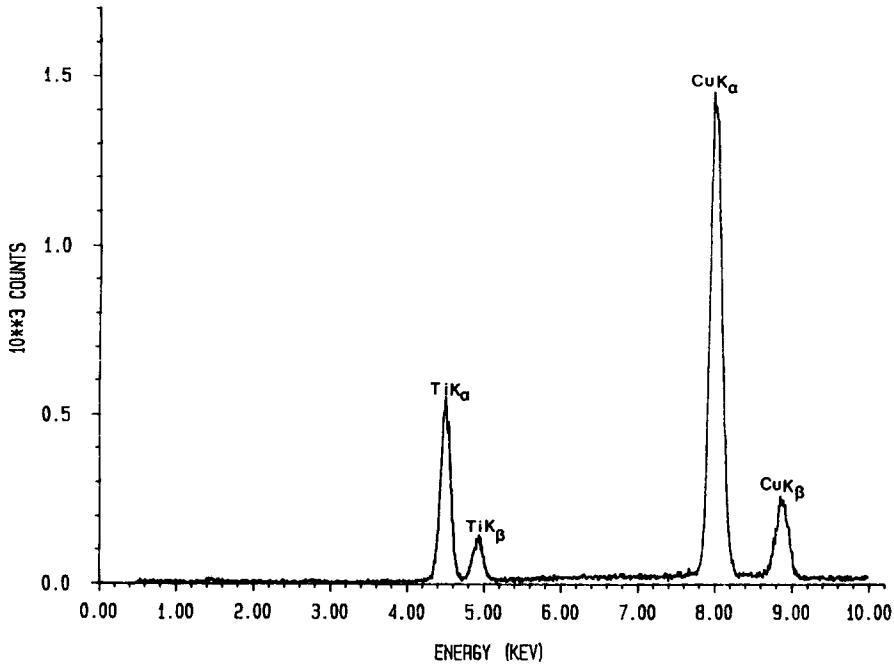

Fig. 6. EDS spectra of a metal free region showing Ti signals only. This is an indication for the presence of metal in the form of discrete islands.

determined by the mean contact area between the grains, A, and the grain diameter, d, e represents the electronic charge, N_c is the effective density of states in the conduction band, E_{cs} represents the conduction band minimum of TiO_2, and E_F is the Fermi energy of the oxide or surface additives. The geometric factors $f(A)$ and $g(d)$ are assumed to be temperature insensitive and are lumped together with other terms in a preexponential factor G_0. Thus,

$$G_i = G_0 \exp\left[-(E_{cs} - E_F)/kT_i\right]. \tag{9}$$

Energetic quantities can be determined on powders in good agreement with single crystal results and do not appear to be controlled by grain boundary effects [21].

For TiO_2 the band gap is reported to be 3.02 eV [22]. An Arrhenius-type plot of conductance G versus inverse temperature was used to determine the difference between E_{cs} and E_F for both the blank TiO_2 chip and the $PtPd/TiO_2$ sample. For blank TiO_2, the Fermi energy level, E_F, was found to be 0.3763 eV below the conduction band minimum of TiO_2, while the presence of Pt and Pd as surface additives narrowed the difference between the conduction band minimum of TiO_2 and the Fermi energy level to 0.0457 eV.

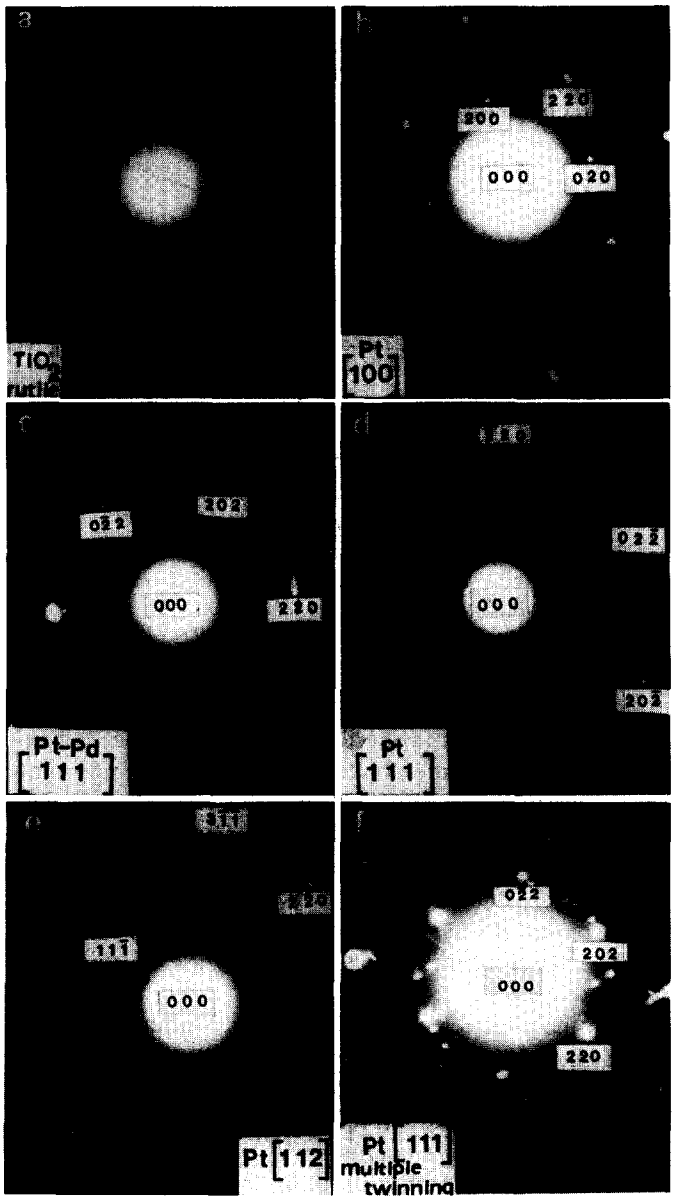

Fig. 7. Electron microdiffraction patterns obtained from different regions of $PtPd/TiO_2$ sample: (a) metal free region, showing ring pattern of rutile, (b) 16 nm particle showing Pt fcc [100] pattern, (c) 10 nm particle showing Pt–Pd alloy formation, fcc zone axis [111], (d) 12 nm particle showing Pt [111] zone axis pattern, (e) 14 nm particle showing Pt [112] zone axis pattern, (f) 8 nm Pt particle showing multiple twinning, Pt zone axis [111].

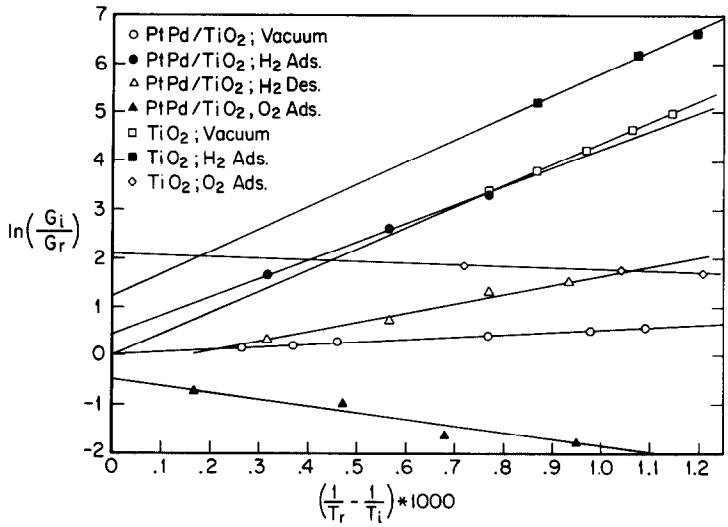

Fig. 8. Arrhenius plots representing normalized data of electrical conductance as a function of reciprocal temperature for PtPd/TiO_2 and blank TiO_2. G_i and G_r are the sample and reference conductance for a given film corresponding to temperatures T_i and T_r, respectively. For PtPd/TiO_2: $T_r = 373$ K, $G_r = 1.585 \times 10^{-3}$ Ω^{-1}. For blank TiO_2: $T_r = 373$ K, $G_r = 6.46 \times 10^{-6}$ Ω^{-1}.

The addition of metal results in more pronounced n-type behavior of TiO_2.

In this analysis, the absolute conductance is not an important parameter, and the Fermi energy level shifts are obtained simply from changes in the slopes of the Arrhenius plots. This treatment effectively eliminates the problems associated with grain boundaries and variable contact areas in pressed powders. The analysis is only valid, however, if the powders have sufficient bulk conductance, and if the surface state density is not a strong function of temperature. The latter condition precludes the use of this method for the study of adsorbed species.

To investigate the effect of gas adsorption on conductance as a function of temperature, Arrhenius plots of conductance versus reciprocal temperature were plotted (fig. 8). As in the case of the thin Pt films, the conductance data were normalized with respect to a reference sample conductance, G_r, measured under vacuum at a reference temperature, T_r.

From the slopes of the Arrhenius plots, apparent activation energies of conductance were determined. Temperature coefficients of resistance, were obtained according to eq. (4). The results are summarized in table 2.

While exposure to H_2 increased the conductance of blank TiO_2, it did not significantly change the apparent activation energy. The effect of H_2 seemed to be completely reversible, as the conductance of the blank TiO_2 could be

Table 2
Activation energies of conductance and temperature coefficients of resistance of TiO_2 and $PtPd/TiO_2$ after treatment in vacuum, H_2 adsorption, H_2 desorption, and treatment in O_2

Sample	Activation energy of conductance (eV) (± 0.002 eV)				Temperature coefficient of resistance (K^{-1}) ($\pm 1\times10^{-4}$)			
	Vacuum	H_2 ads.	H_2 des.	O_2	Vacuum	H_2 ads.	H_2 des.	O_2
TiO_2	−0.376	−0.396	−0.376	0.028	-29.0×10^{-4}	-21.0×10^{-4}	-29.0×10^{-4}	13.6×10^{-4}
$PtPd/TiO_2$	−0.046	−0.368	−0.166	0.115	-13.6×10^{-4}	-29.8×10^{-4}	-32.8×10^{-4}	103.5×10^{-4}

reproduced following evacuation. The increase in conductance might be related to the formation of surface hydroxyl groups resulting in a release of electrons to the conduction band [21,22]. The temperature coefficient of resistance was negative for both the vacuum treated as well as for H_2 treated TiO_2.

Exposure of blank TiO_2 to O_2 resulted in a drastic decrease in conductance, approaching that of insulators. The temperature coefficient of resistance changed sign and became positive. The overall decrease in conductance can be attributed to a filling of anionic vacancies in the TiO_2 by slowly diffusing oxygen. This process is activated, and the diffusion of oxygen will be faster at elevated temperatures. Thus, at higher temperatures, a more efficient filling of vacancies takes place, and the insulator-like behavior of TiO_2 is emphasized. The apparent "positive temperature coefficient of resistance" is the result of the temperature dependence of the diffusion coefficient of oxygen in the solid.

Impregnation of TiO_2 with Pt and Pd led to an increase in conductance by several orders of magnitude. At 373 K, the reference conductance, G_r, of blank TiO_2 was $6.46 \times 10^{-6}\ \Omega^{-1}$, while the PtPd/$TiO_2$ chip had a reference conductance of $1.585 \times 10^{-3}\ \Omega^{-1}$. Since both chips were pressed under identical conditions, starting from powder with identical grain size, it is highly unlikely that differences in contact area and grain boundary effects alone could account for such large differences in the reference conductance. However, it needs to be emphasized that the objective of this study was to measure relative changes in conductance due to gas adsorption, rather than determining absolute values of sample conductance.

Percolation of charge carriers through metal particles on the TiO_2 surface does not seem to be the dominant cause of the observed increase in conductance.

The metal was present on the semiconductor in the form of discrete islands rather than of a coherent layer completely wetting the support via Stranski–Krastanov growth mechanism. The evidence for this comes from electron microscopy and microdiffraction. Transmission electron microscopy (fig. 3) showed the presence of metal particles as regions of high contrast, and X-ray energy dispersive spectroscopy (EDS) indicated patches of TiO_2 which were metal free (fig. 6). Microdiffraction from different regions also indicated the presence of metal free areas (fig. 7a).

The electronic equilibrium at the metal/semiconductor interface is dependent on the relative work function differences between discrete metal islands and the underlying support. Whereas for reduced TiO_x ($x < 2$) with a work function $\phi = 4.6$ eV [25] the direction of electron transfer is from the semiconductor to the metal ($\phi_{Pt} = 5.36$ eV) [26], ($\phi_{Pd} = 4.8$ eV) [23], oxidized TiO_2 ($\phi = 5.5$ eV) [22] tends to inject holes into the metal conduction band. Thus, it is possible to have localized regions with opposite charge transfer characteristic depending on the nature of the metal/semiconductor interface. Chemisorp-

tion on metallic sites would lead to a disruption of the localized equilibrium as it affects the metal work function. In this study, the dissociative chemisorption of H_2 on the metallic sites of $PtPd/TiO_2$ caused a drastic increase in the conductance (fig. 8). This large increase in conductance as compared to thin Pt films on glass (fig. 2) cannot be accounted for by just a charge transfer from hydrogen adatoms to the metal conduction band. The most probable mechanism for this large change in conductance is the spillover of atomic hydrogen from metal sites to the semiconductor and formation of hydroxyl groups with release of free electrons to the conduction band of TiO_2. Such a mechanism has been postulated by Herrmann and Pichat in their study of strong metal support interaction in the Pt/TiO_2 system [21,22]. Desorption of hydroxyl groups as H_2O by combination with atomic hydrogen leaves an anionic-vacancy-rich surface. Consequently, the conductance change during the H_2 adsorption–desorption cycle was not completely reversible for the $PtPd/TiO_2$ catalyst in contrast to thin Pt films on glass where the conductance change was completely reversible in H_2 adsorption/desorption cycles.

The temperature coefficients of conductance, α, of vacuum treated and hydrogen exposed $PtPd/TiO_2$ were negative (table 2), characteristic for an activated process of charge carrier conduction and a further argument against percolation of charge carriers through the metal particles. The latter process, as seen for thin, discontinuous Pt films on glass (table 1) would lead to positive values of α. After adsorption of H_2 on $PtPd/TiO_2$, the value of α became more negative and did not return to its original value upon evacuation (table 2). This behavior was in marked contrast to that of blank TiO_2 where the opposite trend was observed after exposure to H_2 and where evacuation restored the initial value of α.

Exposure of $PtPd/TiO_2$ to O_2 caused a large decrease in conductance which can be attributed to the filling of anionic vacancies in the semiconductor and hole injection in the metal bands (fig. 8, table 2). Particularly noteworthy is the massive change in the temperature coefficient of conductance, α, from a value of $-13.6 \times 10^{-4}\ K^{-1}$ for vacuum treated $PtPd/TiO_2$ to a positive value of $103.5 \times 10^{-4}\ K^{-1}$ upon exposure to oxygen. As in the case of blank TiO_2, this phenomenon can be explained by the temperature dependence of oxygen diffusion, and the filling of anionic vacancies.

Fig. 9 shows the time response of conductance change observed on vacuum treated $PtPd/TiO_2$ upon exposure to either H_2 or O_2 at a temperature of 523 K. Exposure to 800 Pa of H_2 caused a rapid increase in conductance within the first minute. Keeping the chip exposed to H_2 for an additional period of 11 min did not result in any further change in conductance. Removal of H_2 by evacuation decreased the conductance slowly, without reaching the original value of conductance prior to exposure to H_2 gas. At lower temperature (< 423 K) the conductance change was found to be reversible. The fast initial response to H_2 exposure and the lack of complete reversibility of the conduc-

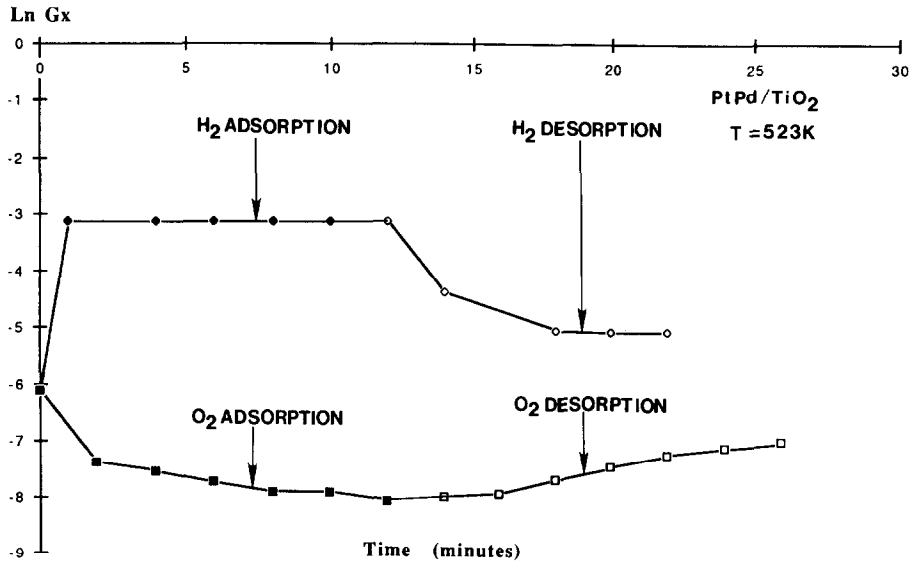

Fig. 9. Time response of conductance change for $PtPd/TiO_2$ sample at 523 K for H_2 and O_2 chemisorption and desorption.

tance change in adsorption/desorption cycles at higher temperatures indicates that not only the metal, but also the TiO_2 substrate must be involved in the adsorption process. It is well known that metals such as Pt adsorb hydrogen dissociatively. At higher temperatures, atomic hydrogen generated on the metal sites becomes mobile and spills over onto the oxide substrate, where it can form hydroxyl groups at the metal/oxide interface. These hydroxyl groups, once formed, are difficult to remove by evacuation, in contrast to chemisorbed hydrogen which can easily be desorbed from metal sites by evacuation at elevated temperatures.

The time response of vacuum treated $PtPd/TiO_2$ to oxygen adsorption was comparatively slow. In contrast to hydrogen exposure, where the conductance quickly reached a final value, the conductance decreased steadily for more than ten minutes and recovered slowly upon evacuation. The slower response to O_2 exposure can be explained in terms of slow diffusion of oxygen into the TiO_2 lattice resulting in the filling of anionic vacancies. Evacuation reverses the process and slowly recreates these anionic vacancies.

In comparison to the Pt films on glass substrates, much larger changes in conductance upon gas chemisorption were found in the $PtPd/Tio_2$ sample. Both systems contain discrete metal islands, and the much more pronounced response to gas adsorption of the $PtPd/TiO_2$ system indicates that the TiO_2 semiconductor participates in chemisorption, thereby contributing to significant changes in charge carrier transport.

4. Conclusions

Thin Pt films supported on glass substrates and $PtPd/TiO_2$ were investigated for the influence of chemisorption on charge carrier transport. Under vacuum, the activation energy for conduction was found to increase as the Pt film thickness decreased and the temperature coefficients of resistance of these thin films were less than that of bulk metal [23]. The low temperature coefficient of resistance of these thin Pt films is due to the small size of Pt particles resulting in shortened mean free path of electrons. H_2 chemisorption on thin Pt films caused an increase in the electrical conductance due to injection of electrons into the metal conduction band. The activation energy for conduction was found to increase as a result of H_2 chemisorption via reduced charge carrier mobility by scattering of conduction band electrons due to adsorbed species. The increase in activation energy for conduction upon chemisorption of H_2 was found to be more pronounced for thicker (> 10 nm) films. This indicates that a higher concentration of adsorbed atoms on thicker films leads to a higher charge carrier scattering, and consequently to more severe reduction in the mobility.

In contrast to the relatively small changes in the conductance of thin Pt films upon H_2 chemisorption, large variations in the conductance were found for $PtPd/TiO_2$. This large change in conductance is believed to be due to the spillover of atomic hydrogen from metal to the semiconductor. The metal Fermi energy level was found to be close to the conduction band minimum of TiO_2 (0.046 eV) permitting a rapid exchange of electrons on the metal/semiconductor interface. Thus, any surface reactivity on the metal had an influence on the surface state energy levels of the semiconductor and vice versa. The long-range percolation of charge carriers through discrete metal islands was not a dominant factor.

The conductance change of $PtPd/TiO_2$ upon chemisorption of H_2 was found to be reversible at lower temperatures (< 423 K). At higher temperatures (> 423 K) the conductance change due to chemisorption became increasingly irreversible during adsorption/desorption cycles as spill-over hydrogen formed hydroxyl groups on the TiO_2 surface which desorbed as water leaving behind a vacancy-rich surface. Oxygen adsorption led to a filling of vacancies in TiO_2 resulting in an insulator-like behavior.

Acknowledgements

Partial financial support for this work through ARO Grant No. DAAG 29-83-K-0131 is gratefully acknowledged. The authors also would like to thank Mr. Peter Severn and Mr. David Klassen for skillful technical assistance.

References

[1] K. Saji, H. Takahashi, H. Kondo, T. Takeuchi and I. Igarashi, in: Chemical Sensors, Vol. 17 of Analytical Chemistry Symposia Series, Eds. T. Seiyama, K. Fueki, J. Shiokawa and S. Suzuki (Elsevier, Tokyo, 1983) p. 171.
[2] E.M. Logothetis and W.J. Kaiser, Sensors Actuators 4 (1983) 333.
[3] M. Katsura, M. Shiratori, T. Takahashi, Y. Yokomizo and N. Ichinose, in: Chemical Sensors, Vol. 17 of Analytical Chemistry Symposia Series, Eds. T. Seiyama, K. Fueki, J. Shiokawa and S. Suzuki (Elsevier, Tokyo, 1983) p. 101.
[4] S.R. Morrison, Sensors Actuators 2 (1982) 329.
[5] M.N. Nifontoff, Compt. Rend. 236 (1953) 538; 237 (1953) 24.
[6] T.E. Hartman, J. Appl. Phys. 34 (1963) 943.
[7] D.S. Herman and T.N. Rhodin, J. Appl. Phys. 37 (1963) 1594.
[8] C.A. Neugebauer and M.B. Webb, J. Appl. Phys. 33 (1962) 74.
[9] I.G. Murgulescu and N.I. Ionescu, Rev. Roumaine Chim. 13 (1968) 1533; 14 (1969) 681, 1073.
[10] I.G. Murgulescu and N.I. Ionescu, Rev. Roumaine Chim. 11 (1966) 1035, 1267; 12 (1967) 1395.
[11] I.G. Murgulescu and N.I. Ionescu, Thin Solid Films 7 (1971) 355.
[12] M. Watanabe, Thin Solid Films 36 (1976) 65.
[13] N.A. Surplice, J. Muller and B. Singh, Thin Solid Films 28 (1975) 179.
[14] Z. Bastl, Surface Sci. 22 (1970) 465.
[15] W.M.H. Sachtler, Surface Sci. 22 (1970) 468.
[16] N. Yamazoe, Y. Kurokawa and T. Seiyama, in: Chemical Sensors, Vol. 17 of Analytical Chemistry Symposia Series, Eds. T. Seiyama, K. Fueki, J. Shiokawa and S. Suzuki (Elsevier, Tokyo, 1983) p. 35.
[17] H. Yanagida, K. Koumoto, M. Miyayama and S. Saito, in: Chemical Sensors, Vol. 17 of Analytical Chemistry Symposia Series, Eds. T. Seiyama, K. Fueki, J. Shiokawa and S. Suzuki (Elsevier, Tokyo, 1983) p. 95.
[18] S.R. Morrison, Sensors Actuators 2 (1982) 329.
[19] B.E. Nieuwenhuys, Surface Sci. 59 (1976) 430.
[20] S.R. Morrison, J. Catalysis 34 (1974) 462.
[21] J.M. Herrmann and P. Pichat, J. Catalysis 78 (1982) 425.
[22] J.M. Herrmann, J. Catalysis 98 (1984) 404.
[23] E. Savitsky, V. Polyakova, N. Gorina and N. Roshan, Physical Metallurgy of Platinum Metals (MIR, Moscow, 1978).
[24] S.R. Morrison, The Chemical Physics of Surfaces (Plenum, New York, 1977) p. 70.
[25] Y.W. Chung, W.J. Lo and G.A. Somorjai, Surface Sci. 64 (1977) 588.
[26] R.C. Weast, Ed., Handbook of Chemistry and Physics (CRC Press, Cleveland, 1972).